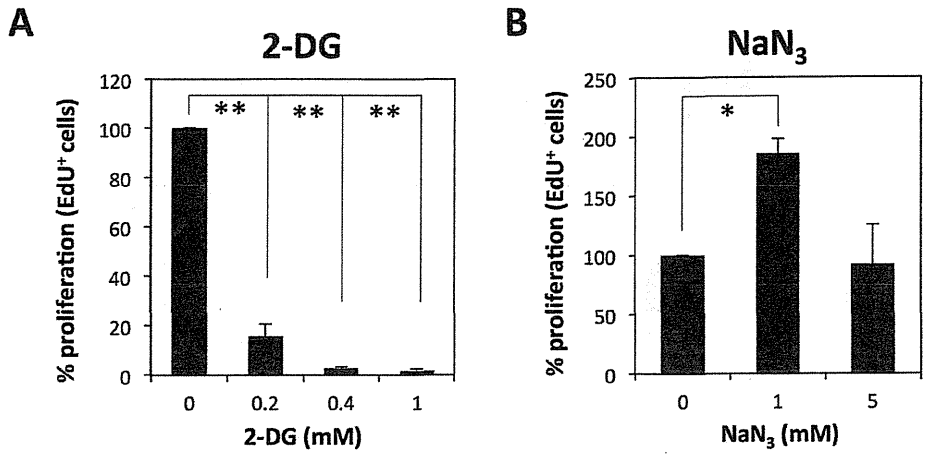

MoriyamaFig7
151x72mm (300 x 300 DPI)

Surg Today (2013) 43:970–976
DOI 10.1007/s00595-013-0528-2

ORIGINAL ARTICLE

Impact of cardiac stem cell sheet transplantation on myocardial infarction

Sfoug Alshammary · Satsuki Fukushima · Shigeru Miyagawa · Takenori Matsuda · Hiroyuki Nishi · Atsuhiro Saito · Sokichi Kamata · Takayuki Asahara · Yoshiki Sawa

Received: 28 June 2012 / Accepted: 2 July 2012 / Published online: 5 March 2013

Abstract
Purpose Myocardial infarction (MI) remains a major cause of mortality because of the limited regenerative capacity of the myocardium. Transplantation of somatic tissue-derived cells into the heart has been shown to enhance the endogenous healing process, but the magnitude of its therapeutic effects is dependent upon the cell-source or cell-delivery method. We investigated the therapeutic effects of C-Kit positive cardiac cell (CSC) cell-sheet transplantation therapy in a rat model of MI.
Methods and results CSCs of human origin were sorted and cultured to generate scaffold-free CSC cell-sheets. One-layered or 3-layered cell-sheets were transplanted into nude rats 1 h after left coronary artery ligation. We observed a significant increase in the left ventricular ejection fraction and a significant decrease in left ventricular systolic dimension at 2 and 4 weeks in the 3-layer group, but not in the 1-layer or sham groups. Consistently, there was less accumulation of interstitial fibrosis in the 3-layer group than in the 1-layer or sham groups. Moreover, capillary density was significantly greater in the 3-layer group than in the 1-layer or sham groups.
Conclusions The 3-layered cell-sheet improved cardiac function associated with angiogenic and anti-fibrotic effects. Thus, CSC is a promising cell-source to use with the cell-sheet method for the treatment of cardiac failure, as long as a sufficient number of cells are delivered.

Keywords Cardiac · Stem cell · Myocardial infarction

S. Alshammary · S. Fukushima · S. Miyagawa · T. Matsuda · H. Nishi · A. Saito · S. Kamata · Y. Sawa (✉)
Department of Cardiovascular Surgery,
Osaka University Graduate School of Medicine,
2-2 Yamadaoka, Suita 565-0871, Japan
e-mail: sawa-p@surg1.med.osaka-u.ac.jp

T. Asahara
Institute of Biomedical Research and Innovation, Kobe, Japan

Introduction

The limited regenerative capacity of the myocardium accounts for the fact that cardiac failure related to myocardial infarction (MI) remains a major cause of morbidity and mortality worldwide, despite major advances in medical and/or interventional treatments [1]. The treatment of cardiac failure relies on strategies that are designed to target and/or limit residual or persistent myocardial ischemia, additional myocardial damage, pathological cardiac remodeling, and hemodynamic impairment, including cardiac dyssynchrony [2]. On the other hand, the transplantation of somatic tissue-derived stem/progenitor cells into the heart has been shown to enhance the endogenous healing process of the damaged myocardium, while the magnitude of the therapeutic effects are dependent on the cell-source, cell-number, cell-delivery method, and target cardiac pathology [3–5]. It has been shown that the transplantation of C-kit-positive heart-derived cells into the MI heart yields functional recovery, mediated by proliferation and differentiation into the heart-composing cells in situ, and by releasing cardioprotective factors that activate native healing processes [6]. However, the optimal preparation and delivery method of CSCs into the heart has not been established.

The cell-sheet method, in which aggregated cells in a sheet shape cultured under a thermoresponsive dish are attached to the epicardial surface [7], has been shown to deliver a large scale of cultured cells with minimal damage to the cells or native cardiac tissues [8]. This enhances its therapeutic effects and minimizes inflammation-related

complications, representing a promising cell-delivery method in CSC transplantation therapy [9]. However, there are concerns about potential ischemia of the implanted cell-sheet, which would limit cellular function, survival, and therapeutic potential. According to a previous study, a 3-layered cell-sheet generated by skeletal myoblasts showed greater therapeutic effects than a 1-layered cell-sheet, while a 5-layered cell-sheet did not enhance the effects, possibly because of ischemia in the implanted cell-sheet [10]. Based on the hypothesis that the therapeutic potential of CSC cell-sheet treatment might be dependent on the number of layers of the cell-sheet, we investigated the therapeutic effects of CSC cell-sheet transplantation therapy on MI hearts using a rat model.

Methods

All studies using human tissues and experimental animals were carried out under approval of the institutional ethical committee. Human tissues were collected only after obtaining written informed consent. This investigation conforms to the Principles of Laboratory Animal Care formulated by the National Society for Medical Research and the Guide for the Care and Use of Laboratory Animals (US National Institutes of Health Publication No. 85-23, revised 1996). All experimental procedures and evaluations were carried out in a blinded manner.

Isolation and culture of C-Kit-positive human cardiac cells and cell-sheet generation

Discarded cardiac tissue samples were taken from the left ventricular apex of a 31-year-old man with dilated cardiomyopathy, requiring daily cardiovascular procedures in Osaka University Hospital. Cardiac cells were dissociated from the tissues, cultured, and then sorted for C-kit using FACSAria (BD Biosciences) to yield C-Kit positive cardiac cells, which were then cultured for expansion with multiple passages. The cells were then incubated in thermoresponsive dishes (35 mm UpCell, CellSeed, Tokyo, Japan) at 37 °C for 2 days prior to transplantation, when the cells were incubated at 25 °C to induce their spontaneous detachment, to yield a mono-layered scaffold-free CSC cell-sheet that included 1.5×10^6 cells (Fig. 1a). The 3-layered cell-sheet was generated by filling up the mono-layered cell-sheet, as described previously [10].

Generation of AMI model and CSC cell-sheet transplantation

Thirty-nine athymic female nude rats, 8 weeks of age, were subjected to permanent ligation of the left coronary artery

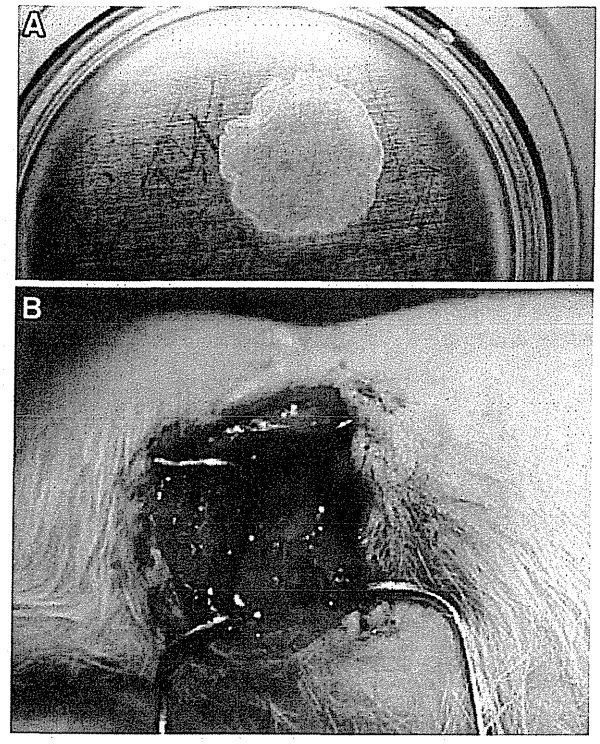

Fig. 1 A mono-layered cell-sheet was generated by c-kit positive cardiac cells of human origin on thermoresponsive dishes in vitro (**a**). A mono-layered or 3-layered cell-sheet was transplanted over the left ventricular free wall of the rat heart, which had been subjected to ischemia by permanent ligation of the corresponding coronary artery, 1 h prior to the treatment (**b**)

(LCA) under general anesthesia with endotracheal intubation and isoflurane inhalation, as previously described [10]. LCA ligation-related death occurred prior to treatment in 16 %. The rats that survived for 50 min after the ligation were randomly assigned to the following three treatment groups: transplantation of a 3-layered cell-sheet ($n = 12$), transplantation of a l-layered cell-sheet ($n = 10$), or a sham operation ($n = 11$). In the two transplantation groups, the cell-sheet was attached directly to the epicardial surface of the ischemic/infarct area (Fig. 1b) [10]. The cell-sheet was large enough to cover all of the ischemic or infarcted area. By 20 min after the transplantation, when the cell-sheets were properly fixed to the cardiac surface, the chest was closed and the rats were allowed to recover in individual temperature-controlled cages until they were killed 28 days after the treatment.

Transthoracic echocardiography

Transthoracic echocardiography was performed under isoflurane inhalation, using a system equipped with a 12 MHZ transducer (GE Healthcare). Diastolic and systolic dimensions of the left ventricular diastolic and

systolic dimensions (LVDD and LVDS, respectively) were measured at the papillary muscle level by the M-mode, while the LV ejection fraction (LVEF) was calculated by the following formula: $(LVDD^3–LVDS^3)/LVDd^3 \times 100$ [10, 11].

Histology

The ventricles were immerse-fixed in 4 % paraformaldehyde, embedded in paraffin, and cut into 5 micrometres using a microtome for histological studies. The sections were stained by hematoxylin–eosin (HE) or Masson trichrome (MT) and assessed by optical microscopy (Olympus, Tokyo, Japan). Metamorph software was used to separate stained and non-stained myocardium by MT staining and to quantitatively calculate each area. The sections were labeled immunohistologically by polyclonal anti-von Willebrand factor antibody (vWF, DAKO, Glostrup, Denmark), and visualized by the LSABTM kit (DAKO), which is an automated immunostaining system based on the LSAB Lepto strept avidin–biotin-peroxidase method. The sections were labeled immunohistologically by the anti-human-specific HLA antibody or anti-cardiac troponin (cTn) I antibody, visualized by corresponding secondary antibodies that were counterstained by DAPI, and assessed by confocal microscopy (Olympus).

Statistics

Values are expressed as mean ± SEM. The three groups were compared with 1-way or 2-way ANOVA as appropriate, followed by the Fisher protected least-significant difference test, or the Kruskal–Wallis test, followed by the post hoc pairwise Wilcoxon-Mann–Whitney U test, as appropriate. Differences were considered significant at $P < 0.05$. All analyses were performed using SPSS for Windows (SPSS, Chicago, IL, USA).

Results

Functional recovery following CSC cell-sheet transplantation

Scaffold-free CSC cell-sheet was prepared from primary C-kit positive cardiac cells of human origin, cultivated in thermoresponsive dishes. We transplanted the 1-layered or 3-layered cell-sheets onto the epicardial surface of the nude rat 1 h after the permanent LCA ligation. A sham operation was performed for the control group. Cardiac performance was serially assessed by transthoracic echocardiography just after the treatment (baseline), and then 1, 2, and 4 weeks after the treatment.

Before any intervention, the LVEF, LVDD, and LVDS did not differ significantly among the groups (Fig. 2). However, for 4 weeks after treatment, the LVEF showed a significantly progressive reduction, while the LVDD and LVDS showed a significantly progressive increase in the sham group and the 1-layer group. Conversely, in the 3-layer group, the LVEF showed a significant increase, and the LVDS showed a significant decrease 2 and 4 weeks following the transplantation, while the LVDD did not change significantly in this group over the 4 weeks. Notably, the LVEF in the 3-layer group was significantly greater than that in the 1-layer group or sham group, while the LVDS in the 3-layer group was significantly lower than that in the 1-layer group or sham group. The LVDD did not differ significantly among the groups at any time.

Histological reverse LV remodeling following CSC cell-sheet transplantation

We assessed gross structure, interstitial fibrosis and capillary distribution in the myocardium 4 weeks after the CSC cell-sheet transplantation to qualitatively and semi-quantitatively explore the degree of LV remodeling in each group by HE staining, Masson Trichrome staining, and immunohistolabelling for von Willebrand factor, respectively. The infarcted area, in which the cell-sheet was transplanted, was clearly thicker in the 3-layer group than in the 1-layer or sham groups, as assessed by the HE staining (Fig. 3a–c). In addition, the myocardial structure in the peri-infarcted area was better preserved in the 3-layer group than in the 1-layer group or the sham group. There seemed to be less accumulation of interstitial fibrosis in the peri-infarcted and infarct-remote myocardium of the 3-layer group than in the 1-layer group or sham groups (Fig. 3d–f). In fact, computer-based morphometry confirmed significantly less fibrosis in the 3-layer groups than in the 1-layer group or sham group (Fig. 4a). Capillary density in the peri-infarcted myocardium was significantly greater in the 3-layer group than in the 1-layer group or sham group (Fig. 4b).

Phenotypic fate of the transplanted CSCs in the heart

The transplanted CSCs in the heart were phenotypically assessed by immunohistolabelling for human-specific HLA, which clearly dissected the transplanted cells in the native cardiac tissue. While the transplanted cells were rarely present in the 1-layer group 4 weeks after transplantation, the 3-layer group showed abundant human-specific HLA-positive transplanted cells in the tissues epicardially attached to the native cardiac tissue, which were assumed to consist of the remaining transplanted cell sheet and accumulated cells of native origin (Fig. 5a).

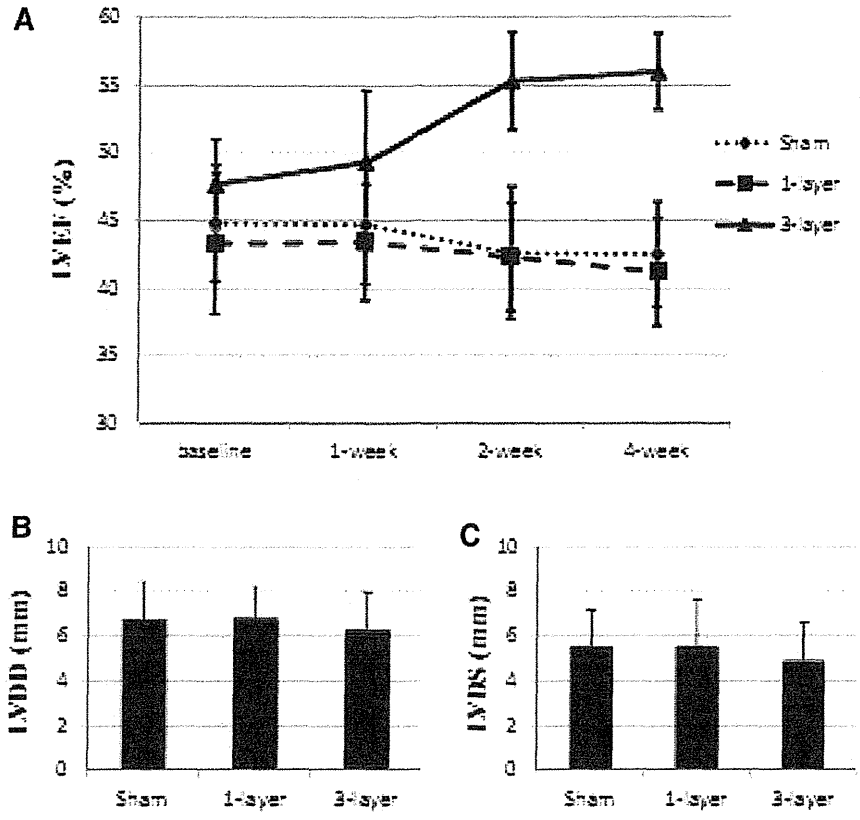

Fig. 2 Cardiac performance measures, such as left ventricular ejection fraction (LVEF) (**a**), LV diastolic dimension (LVDD, **b**), and LV systolic dimension (LVDS, **c**), were assessed echocardiographically immediately after treatment and then 1, 2, and 4 weeks after treatment (sham operation vs. 1-layer cell-sheet transplantation vs. 3-layer cell-sheet transplantation)

Notably, some human-specific HLA-positive transplanted cells were present in the native myocardium, suggesting the migration of transplanted cells into the native cardiac tissue (Fig. 5b–d).

Discussion

This study demonstrated clearly that the transplantation of CSC cell-sheets to treat the MI heart yielded significant recovery of cardiac performance in a cell-sheet layer dependent manner. Consistently, the hearts transplanted with the multi-layered cell-sheet showed significantly more preserved gross myocardial structure, reduced interstitial fibrosis, and increased capillary density than the hearts transplanted with a mono-layered cell-sheet. Moreover, the differentiation of heart-composing cells, including cardiomyocytes, endothelial cells, and vascular smooth muscle cells, was greater in the hearts transplanted with the multi-layered cell-sheet than in those transplanted with the mono-layered cell-sheet.

The transplanted cell-source is known to be a major determinant of the therapeutic effects of cell transplantation therapy for cardiac failure [10–12]. The transplantation of skeletal myoblast transplantation predominates anti-fibrotic effects, whereas that of bone marrow-derived cell transplantation predominates neoangiogenesis in the ischemic/infarcted myocardium. These effects are mediated by indirect effects, in which cell transplantation upregulates a variety of cardioprotective factors to enhance the native healing process, although differentiation of the transplanted cells into the functional heart-composing cells, such as cardiomyocytes or vascular cells rarely occur following the transplantation of skeletal myoblasts or bone marrow-derived cells [13, 14]. In contrast, the transplantation of CSCs has been shown to yield therapeutic effects both directly and indirectly [15, 16]. This study showed that the transplantation of CSCs induced both anti-fibrotic and neoangiogenic effects in a transplanted cell number-dependent manner, indicating that CSCs might have released soluble factors to activate the anti-fibrotic and angiogenic process of the native myocardium following the transplantation. Moreover, the differentiation into the cardiomyocytes and vascular cells, shown in this study, suggests potential direct contribution of these cells to functional recovery, although the magnitude of these direct effects on the global cardiac function remains unclear.

The number of transplanted cells is also an important contributor to the therapeutic effects. Although the cell-sheet method has been shown to deliver more cells into the heart than other delivery methods, such as intramyocardial or intracoronary injection [10], ischemia in the transplanted

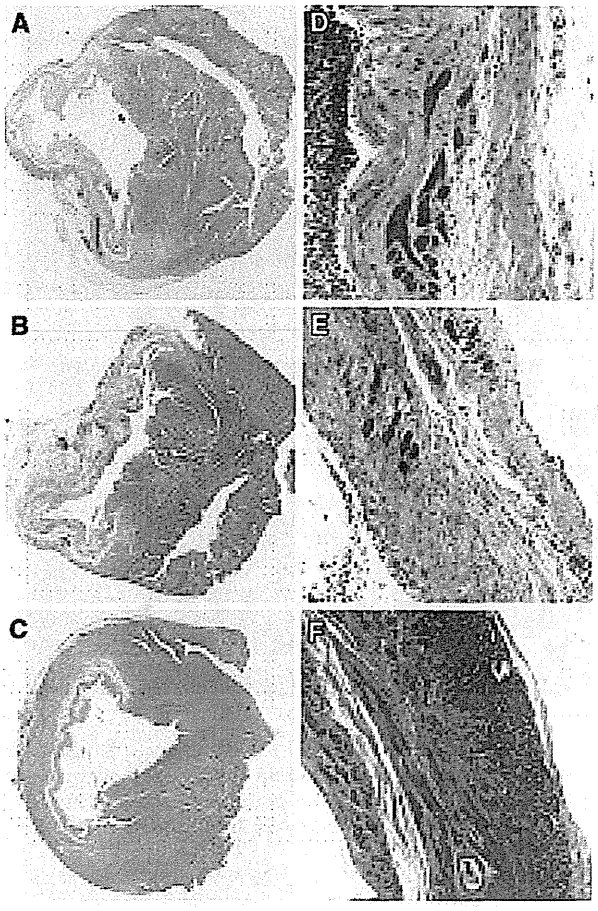

Fig. 3 The gross structure of the heart 4 weeks after treatment was assessed by H&E staining. The sham group (**a**) and the 1-layer group (**b**) showed a large infarcted area in the left ventricular (LV) free wall, but the 3-layer group (**c**) showed a better preserved LV free wall. Interstitial fibrosis 4 weeks after the treatment was assessed by Masson Trichrome staining, which showed more accumulated fibrosis in the sham group (**d**) and the 1-layer group (**e**) than in the 3-layer group (**f**)

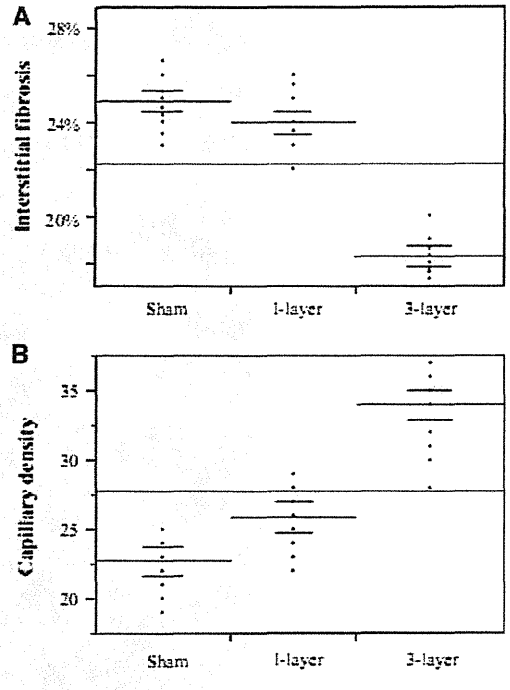

Fig. 4 Masson Trichrome staining revealed a significantly lower percentage of fibrosis 4 weeks after the treatment in the 3-layer group than in the sham or 1-layer groups ($P < 0.05$ vs. the sham and the 1-layer group). Capillary density 4 weeks after treatment, assessed by immunohistochemistry for von Willebrand factor, was significantly greater in the 3-layer group than in the sham or 1-layer groups ($P < 0.05$ vs. the sham and the 1-layer group)

cell-sheet might be a critical limiting factor to the effects. In fact, it was reported that ischemia-related cell-necrosis occurs in the transplanted cells in accordance with the number of cell-sheets filled up [10, 17]. Furthermore, our researchers reported previously that the therapeutic effects of skeletal myoblast cell-sheets increased with the number of layers, but plateaued at five layers, possibly because of ischemia-related functional impairment of the transplanted cell-sheet, although skeletal myoblasts are known to be highly resistant to ischemic stimuli [10, 18, 19]. This study showed that the therapeutic effects of the CSC cell-sheet increased up until three layers, despite poor vascular support after acute infarction of the cell-sheet transplanted area, warranting 3-layered CSC cell-sheet transplantation for treating ischemia-related cardiac failure. Integration of the transplanted CSC cell-sheet into the native myocardium is also a concern of this treatment, as the cell-sheet was simply attached to the epicardial surface. However, this study unveiled that the transplanted cells migrated into the native myocardium and differentiated to heart-composing cells, although the biological mechanisms of this migration process remain unclear.

This study is limited by fact that we used a rodent model transplanted with cells of human origin. The difference in factors related to biological actions between the rat and the human might have modulated the therapeutic effects of this treatment, although a number of previous reports would justify using this model to mimic the clinical scenario [17, 20]. Moreover, using the cells from one patient in the in vivo study might not be appropriate to investigate the effects of CSC of human origin in general, although the cellular behavior did not seem to differ among more than five patients in vitro (data not shown), in accordance with previous reports [21].

In conclusions, the 3-layered cell-sheet improved cardiac function associated with angiogenic and anti-fibrotic effects in a rat model. Thus, the delivery of a sufficient number of CSCs by a cell-sheet method represents a promising treatment for cardiac failure, although further optimization is essential.

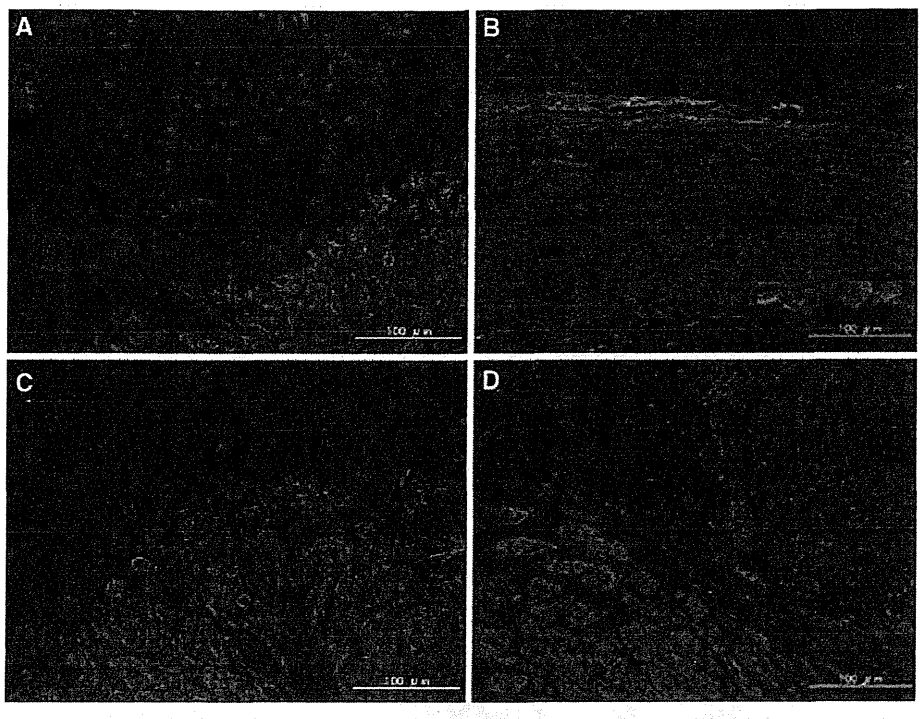

Fig. 5 The presence and distribution of transplanted CSCs of human origin were immunohistologically assessed using human-specific anti-HLA antibody. By 4 weeks after transplantation, the 3-layer group showed abundant human-specific HLA-positive transplanted cells in tissues that were epicardially attached to the native cardiac tissue (**a**). Some human-specific HLA-positive transplanted cells were present in the interstitium of the native myocardium (**b–d**)

Conflict of interest There are no relationships or conflicts of interest related to this manuscript.

References

1. Braunwald E, Bristow M. Congestive heart failure: fifty years of progress. Circulation. 2000;102:14–23.
2. Kania G, Boheler KR, Landmesser U, Wojakowski W. Stem cells in heart failure. Stem Cells Int. 2011 [Epub Nov30].
3. Robey TE, Saiget MK, Reinecke H, Murry CE. Systems approaches to preventing transplanted cell death in cardiac repair. J Mol Cell Cardiol. 2008;45:567–81.
4. Giraud MN, Armbruster C, Carrel T, Tevaearai HT. Current state of the art in myocardial tissue engineering. Tissue Eng. 2007;13: 1825–36.
5. Jawad H, Ali NN, Lyon AR, Chen QZ, Harding SE, Boccaccini AR. Myocardial tissue engineering. Br Med Bull. 2008;87:31–47.
6. Beltrami AP, Barlucchi L, Torella D, Baker M, Limana F, Chimenti S, et al. Adult cardiac stem cells are multipotent and support myocardial regeneration. Cell. 2003;114:763–76.
7. Shimizu T, Yamato M, Kikuchi A, Okano T, et al. Two-dimensional manipulation of cardiac myocyte sheets utilizing temperature-responsive culture dishes augments the pulsatile amplitude. Tissue Eng. 2001;7:141–51.
8. Sawa Y, Miyagawa S, Sakaguchi T, Fujita T, Matsuyama A, Saito A, Shimizu T, Okano T. Tissue engineered myoblast sheets improved cardiac function sufficiently to discontinue LVAS in a patient with DCM: report of a case. Surg Today. 2012;42:181–4.
9. Shimizu T, Yamato M, Kikuchi A, Okano T. Cell sheet engineering for myocardial tissue reconstruction. Biomaterials. 2003;24:2309–16.
10. Sekiya N, Matsumiya G, Miyagawa S, Saito A, Shimizu T, Okano T, et al. Layered implantation of myoblast sheets attenuates adverse cardiac remodeling of the infarcted heart. J Thorac Cardiovasc Surg. 2009;138:985–93.
11. Imanishi Y, Miyagawa S, Maeda N, Fukushima S, Kitagawa-Sakakida S, Daimon T, et al. Induced adipocyte cell-sheet ameliorates cardiac dysfunction in a mouse myocardial infarction model: a novel drug delivery system for heart failure. Circulation. 2011;124:S10–7.
12. Zakharova L, Mastroeni D, Mutlu N, Molina M, Goldman S, Diethrich E, et al. Transplantation of cardiac progenitor cell sheet onto infarcted heart promotes cardiogenesis and improves function. Cardiovasc Res. 2010;87:40–9.
13. Forte E, Chimenti I, Barile L, Gaetani R, Angelini F, Ionta V, et al. Cardiac cell therapy: the next (re)generation. Stem Cell Rev. 2011;7:1018–30.
14. Tongers J, Losordo DW, Landmesser U. Stem and progenitor cell-based therapy in ischaemic heart disease: promise, uncertainties, and challenges. Eur Heart J. 2011;32:1197–206.
15. Kawaguchi N, Smith AJ, Waring CD, Hasan MK, Miyamoto S, Matsuoka R, et al. c-kitpos GATA-4 high rat cardiac stem cells foster adult cardiomyocyte survival through IGF-1 paracrine signaling. PLoS ONE. 2010;5:e14297.
16. Rota M, Padin-Iruegas ME, Misao Y, De Angelis A, Maestroni S, Ferreira-Martins J, et al. Local activation or implantation of cardiac progenitor cells rescues scarred infarcted myocardium improving cardiac function. Circ Res. 2008;103:107–16.
17. Shudo Y, Miyagawa S, Fukushima S, Saito A, Shimizu T, Okano T, et al. Novel regenerative therapy using cell-sheet covered with omentum flap delivers a huge number of cells in a porcine myocardial infarction model. J Thorac Cardiovasc Surg. 2011;142: 1188–96.
18. Hata H, Matsumiya G, Miyagawa S, Kondoh H, Kawaguchi N, Matsuura N, et al. Grafted skeletal myoblast sheets attenuate myocardial remodeling in pacing-induced canine heart failure model. J Thorac Cardiovasc Surg. 2006;132:918–24.
19. Memon I, Sawa Y, Fukushima N, Matsumiya G, Miyagawa S, Taketani S, et al. Repair of impaired myocardium by means of implantation of engineered autologous myoblast sheets. J Thorac Cardiovasc Surg. 2005;130:1333–41.

20. Tang Y. Cellular therapy with autologous skeletal myoblasts for ischemic heart disease and heart failure. Methods Mol Med. 2005;112:193–204.

21. He J, Vu D, Hunt G, Chugh A, Bhatnagar A, Bolli R. Human cardiac stem cells isolated from atrial appendages stably express c-kit. PLoS ONE. 2011;6:e27719.

Hindawi Publishing Corporation
BioMed Research International
Volume 2013, Article ID 583912, 6 pages
http://dx.doi.org/10.1155/2013/583912

Hindawi

Review Article

Present and Future Perspectives on Cell Sheet-Based Myocardial Regeneration Therapy

Yoshiki Sawa and Shigeru Miyagawa

Department of Cardiovascular Surgery, Osaka University Graduate School of Medicine E1, 2-2 Yamadaoka, Suita, Osaka 565-0871, Japan

Correspondence should be addressed to Yoshiki Sawa; sawa@surg1.med.osaka-u.ac.jp

Received 4 October 2013; Accepted 28 October 2013

Academic Editor: Ryuichi Morishita

Heart failure is a life-threatening disorder worldwide and many papers reported about myocardial regeneration through surgical method induced by LVAD, cellular cardiomyoplasty (cell injection), tissue cardiomyoplasty (bioengineered cardiac graft implantation), *in situ* engineering (scaffold implantation), and LV restrictive devices. Some of these innovated technologies have been introduced to clinical settings. Especially, cell sheet technology has been developed and has already been introduced to clinical situation. As the first step in development of cell sheet, neonatal cardiomyocyte sheets were established and these sheets showed electrical and histological homogeneous heart-like tissue with contractile ability *in vitro* and worked as functional heart muscle which has electrical communication with recipient myocardium in small animal heart failure model. Next, as a preclinical study, noncontractile myoblast sheets have been established and these sheets have proved to secrete multiple cytokines such as HGF or VEGF *in vitro* study. Moreover, *in vivo* studies using large and small animal heart failure model have been done and myoblast sheets could improve diastolic and systolic performance by cytokine paracrine effect such as angiogenesis, antifibrosis, and stem cell migration. Recently evidenced by these preclinical results, clinical trials using autologous myoblast sheets have been started in ICM and DCM patients and some patients showed LV reverse remodelling, improved symptoms, and exercise tolerance. Recent works demonstrated that iPS cell-derived cardiomyocyte sheet were developed and showed electrical and microstructural homogeneity of heart tissue *in vitro*, leading to the establishment of proof of concept in small and large animal heart failure model.

1. Introduction

Therapeutic treatments using cells or cell-based tissues have been developed to regenerate the damaged myocardium associated with ischemic heart disease. This technique has already been evaluated in the clinical setting, using myoblasts [1] or bone marrow mononuclear cells (BM-MNCs) [2]. Although these studies demonstrated the feasibility and safety of this approach, the efficacy associated with this technology was generally insufficient to repair severe myocardial damage. Thus, a second generation of myocardial regenerative therapy, tissue-engineered cardiomyoplasty, is currently being developed. A large number of achievements concerning basic, preclinical, and clinical works about cell sheet technology have been done and this review summarizes recent advances in myocardial regeneration emerging from the development of cell sheet technology.

2. Development of Cell Sheet Technology

Cell-sheet techniques have been applied to several diseased organs, such as the heart [3], eye [4], and kidney [5], in the laboratory and the clinic. Cell sheets can be prepared on special dishes that are coated with a temperature-responsive polymer, poly(N-isopropylacrylamide) (PIPAAm), that changes from being hydrophobic to hydrophilic when the temperature is lowered. This change allows cells to be removed without EDTA or enzymatic treatment and without destroying the cell-cell or cell-extracellular matrix (ECM) interactions within the cell sheet.

Shimizu et al. used such temperature-sensitive culture dishes to develop a contractile chick cardiomyocyte sheet that exhibited a recognizable heart tissue-like structure and showed electrical pulsatile amplitude [6]. Next, they layered single-cell sheets to generate bilayer-cell sheets, forming an electrically communicative three-dimensional cardiac construct, which exhibited spontaneous and synchronous pulsation with electrical communication between the cell sheets, mediated by connexin 43. Furthermore, the cell sheets adhered together rapidly, as indicated by the presence of desmosomes and intercalated disks between them [7]. When the pulsatile cardiac tissue was implanted subcutaneously, it was found to assume a heart tissue-like structure and exhibited neovascularization and spontaneous beating for up to one year. The size, conduction velocity, and contractile force of the engrafted sheets increased in proportion to the host growth [8, 9].

Miyagawa et al. demonstrated that a neonatal cardiomyocyte sheet could communicate electrically with the host myocardium, as indicated by the presence of connexin 43, and changes in the QRS wave and action potential amplitude, leading to improved cardiac performance in a rat model of ischemic heart disease [3]. This study clearly showed electrical and morphological coupling between the cell sheet and host myocardium and that the cell sheet could contract synchronously with the beating of the host heart and improve the regional systolic function.

A detailed analysis of the vascularization process following cell sheet implantation was undertaken by Sekiya et al. These authors reported that the cardiomyocyte sheet expresses angiogenesis-associated genes and forms an endothelial cell network. Evidence was also presented suggesting that the vessels arising in the engrafted sheet migrate to connect with the host vasculature [10].

Myocardial tissue grafts engineered with cell sheet technology represent a promising therapy for repairing the damaged myocardium, but there may be some inherent limitations. For example, cellular treatment for heart failure may be not suitable for emergency situations. Another issue is that wide therapeutic use will require improvement in the uniformity in the quality of the cultured cells.

Recently, new medications that imitate the paracrine effects of cytokines in cell sheets have been reported, and the addition of such medications could improve the regenerative treatment for heart failure. It was reported that the direct introduction of a prostacyclin agonist into the damaged myocardium induced significant functional recovery in a canine model of dilated cardiomyopathy, via the upregulation of multiple cytokines, including HGF, VEGF, and SDF-1 [11]. Similarly, the implantation of an atelocollagen sheet containing a prostacyclin analogue induced improved cardiac function and a prolonged survival rate in a mouse model of acute myocardial infarction, accompanied by an enhanced expression of SDF-1 [12]. Recent work has also revealed that prostacyclin may be upregulated in the implanted myoblast sheet in the early phases after implantation in response to ischemic conditions and may in turn stimulate endothelial or smooth muscle cells to secrete multiple cytokines including HGF, VEGF, and SDF-1 (data not shown).

3. Experimental and Clinical Work on Myoblast Sheets

In the clinical setting, cellular cardiomyoplasty is reported to have potential regenerative capability, and a method using skeletal myoblasts has been evaluated in clinical trials and found to be relatively feasible and safe [13]. For tissue cardiomyoplasty, skeletal myoblasts are the cell source closest to being ready for clinical application at this time. Memon et al. demonstrated that the nonligature implantation of a skeletal myoblast sheet into a rat cardiac ligation model regenerated the damaged myocardium and improved global cardiac function, by attenuating cardiac remodeling via hematopoietic stem-cell recruitment and growth-factor release, with better restoration of the implanted cells than that obtained using needle injection [14]. In another study, the application of a skeletal myoblast sheet into a 27-week dilated cardiomyopathy hamster model resulted in the attenuated deterioration of cardiac performance accompanied by the preservation of alpha-sarcoglycan and beta-sarcoglycan expression in the host myocytes, and an inhibition of fibrosis, leading to prolonged survival rates [15]. In addition, the grafting of skeletal myoblast sheets attenuated cardiac remodeling and improved cardiac performance in a pacing-induced canine heart failure model [16]. Studies from our group have shown that myoblast sheets may improve cardiac performance via cytokines such as HGF or VEGF (XX).

The mechanism of recovery in the damaged myocardium has not been completely elucidated and may be very complicated. As mentioned above, cytokine release and hematopoietic stem-cell recruitment are possible mechanisms of regeneration; however, other regenerative mechanisms are likely to be involved as well. Skeletal myoblasts cannot beat synchronously with the host myocardium *in vitro* [17] or *in vivo* [18], and, thus, they do not appear to be functionally integrated. However, data from our human and porcine studies suggested that after myoblast sheet implantation, the diastolic dysfunction in the distressed region of the myocardium was significantly recovered compared with controls, leading to improved systolic function in the same region, without contraction of the implanted myoblasts (data not shown). Massive angiogenesis in the implanted region was detected histologically and appeared to be a critical feature associated with the improvement. Thus, we speculate that angiogenesis and the recovery of diastolic function are both major components of the regenerative mechanism in myoblast sheet implantation [19].

On the other hand, immunohistochemical analysis has indicated that the myoblast sheet may only survive for a few months after implantation. We speculate that in the early phases after implantation of the myoblast sheet, the ischemic conditions induce the upregulated expression of several cytokines by the myoblasts that promote their own survival. These cytokines then in turn enhance angiogenesis and the recruitment of stem cells, leading to improved blood perfusion to reactivate the damaged myocardium. The system may continue to be effective in spite of the short-lived myoblast sheet, due to long-term maintenance of the newly developed vasculature.

We recently initiated a clinical evaluation of autologous myoblast sheet implantation. We tested the technology in four patients who were using left ventricular assist devises (LVADs); three of the four patients showed functional recovery, and in two of the patients, the treatment provided a bridge to recovery [20]. Six years later, these two patients have no symptoms of heart failure. We have also implanted myoblast sheets into eight patients with ischemic cardiomyopathy and seven with dilated cardiomyopathy (who were not using LVADs). In that study, some of the patients exhibited left ventricle reverse remodeling and improvements in exercise tolerance and symptoms, with no major adverse cardiac events (MACEs) (data not shown). This clinical research program is ongoing, as we continue to evaluate patients with dilated cardiomyopathy and ischemic cardiomyopathy with and without the use of LVADs.

4. Other Types of Cell Sheets

In addition to cardiomyocytes and myoblasts, other types of cell sheets have been used effectively to improve cardiac performance. The transplantation of a mesenchymal stem cell (MSC) sheet onto the infarcted myocardium of rats resulted in increased anterior wall thickness and new vessel formation, accompanied by a low incidence of differentiation of the implanted cells to cardiomyocytes [21]. While the small number of differentiated cardiomyocytes may not have contributed to the observed improvement in systolic function in this study, the cell sheet exhibited self-propagating properties that promoted the generation of a thick-layered sheet. Although the MSC sheet exhibited a maximum thickness of approximately 600 μm, which would not be strong enough to correct human end-stage heart failure [22], this method of self-propagation is a potential strategy for creating a thick-layered sheet *in vivo*, with the potential for cardiac tissue regeneration.

A further development in cell sheet technology is the creation of a cell sheet composed of two types of cocultured cells; this type of cell sheet was developed to enhance angiogenesis [23, 24]. The cocultured cell sheet, which combined fibroblasts and endothelial progenitor cells, enhanced blood vessel formation and led to functional improvement in a rat myocardial infarction model [24]. Cocultured cell sheets combining fibroblasts and human smooth muscle cells were found to accelerate the secretion of angiogenic factors *in vitro* and to increase blood perfusion *in vivo* by the formation of new vessels [25]. This enhanced effectiveness attained by coculturing two cell types is supported by another study in which the coimplantation of BMCs and myoblasts showed improved results compared to the transplantation of a single cell type in a canine model of ischemic cardiomyopathy [26].

Cell sheets composed of stem cell antigen-1- (sca-1-) positive, or kit-positive cells may represent additional promising approaches. Matsuura et al. demonstrated that sca-1-positive cell sheets could differentiate into cardiomyocytes *in vivo* and produce VCAM-1, leading to improved cardiac performance in a mouse model of myocardial infarction [27]. The administration of c-kit-positive stem cells has shown efficacy in animal models of cardiac dysfunction, and this approach is currently being tested in clinical trials in combination with coronary artery bypass grafting, with encouraging preliminary results [28]. In another study, a c-kit-positive cell sheet combined with endothelial progenitor cell injection was found to induce better functional recovery of endocardial scar tissue than that induced by the cell sheet alone, despite the poor transdifferentiation ability of the c-kit-positive cells into cardiomyocytes [29].

Many of the cell sources mentioned above demonstrate regenerative ability based on the paracrine effect of secreted cytokines; however, newly differentiated cardiomyocytes may be the best candidate cells to regenerate the damaged myocardium. In 2006, Takahashi and Yamanaka reported the development of induced pluripotent stem (iPS) cells that can differentiate into various types of cells, such as cardiomyocytes, cartilage, and nerve cells [30]. Since then, there have been many reports showing that cardiomyocytes derived from iPS cells demonstrate electrophysiological, functional, and microstructural similarities to native cardiomyocytes [31]. Cardiomyocyte sheets derived from human or mouse iPS cells that contract synchronously *in vitro* have been developed, and studies indicate that these cardiomyocyte sheets can contract *in vivo* as analyzed by X-ray diffraction with synchrotron radiation. The transplantation of these sheets leads to functional recovery with upregulated electrical potential in the scarred areas in large [32] and small animal myocardial infarction models [33].

Although preclinical studies appear promising, the safety of these artificially generated cells must be evaluated thoroughly before they can be used in the clinic. In addition, a potential limitation of iPS cell-derived cardiomyocytes may be the loss of cardiomyocytes due to ischemia after implantation. Recent studies have proposed supplemental strategies to avoid ischemia. In one study, the combination of an iPS-derived cardiomyocyte sheet with omentum, which has a rich vasculature network, resulted in retention of the implanted cardiomyocytes and enhanced functional recovery compared with the cardiomyocyte sheet alone [34]. In another study, the transplantation of a cardiomyocyte sheet containing iPS cell-derived endothelial cells led to enhanced functional recovery in a rat myocardial infarction model and increased survival of the implanted cardiomyocytes [35]. Thus, to successfully treat the severely damaged myocardium using iPS cell-derived cardiomyocyte sheets, additional strategies to increase angiogenesis and reduce ischemia may be required.

5. Advantages of Cell Sheet Technology

Studies on the original myoblast cell therapy, in which cells were directly injected into the myocardium, indicated that the proportion of injected cells surviving to engraft the infarcted myocardium was too low to be effective. This low level of engraftment may have been caused by the injected cells leaking out of the injected region and being carried to other organs, or due to mechanical stress resulting in cellular loss of function. The resulting rapid cell loss [14] limited the usefulness of the original myoblast cell therapy.

To overcome the problems associated with the intramyocardial injection of cells, many investigators have combined cell transplantation with protein or gene therapy [36], or with tissue-engineered techniques [3]. We have also developed a new cell delivery system that uses tissue-engineered myoblast grafts grown as cell sheets and have utilized animal studies to guide clinical trials. These studies showed that the viability of the transplanted cells was higher than that of injected cells, and that the transplanted myoblasts survived for at least 3 months in the cardiac tissue of a porcine model of heart failure treated with autologous myoblast sheets. Using tissue-engineered temperature responsive techniques, we found that the implanted cells could be applied in larger numbers, were viable during transplantation, and were not lost from the applied region. Furthermore, we showed that cell sheets could be engrafted onto the failed myocardium and contribute to the attenuation of cardiac dysfunction and remodeling [14].

In cell therapy for cardiac disease, life-threatening adverse events involving arrhythmogenicity are a potential risk in both animal models and human clinical trials [37]; however, life-threatening arrhythmias have not been observed during the clinical course of patients who have received autologous cell sheet transplants. In any case, arrhythmias can occur during the natural clinical course of severe heart failure, so their cause may not be easily determined. Procedures using needle injection may cause scars in the myocardium that could in turn induce arrhythmias. Our cell delivery techniques using cell sheets prepared on temperature-responsive culture dishes may carry less risk for the induction of arrhythmias. Myoblasts have a weak electrical potential, and it may be possible for these cells to induce arrhythmia if they survive in the myocardium. However, cell sheets may not be able to induce arrhythmia, since they are attached to the epicardium.

Another potential problem is the limited blood perfusion to the implanted cell sheets. Although the survival of implanted cells using the cell sheet technique has already been shown to exceed the cell survival using other delivery routes, the survival rate was still found to be relatively low when the cells were implanted on the epicardium with this technique [38]. Although we have reported that improved cardiac performance depends on the dose of implanted myoblast sheets, the use of too many cell sheets results in a reduced blood supply. Thus, additional strategies, such as combining myoblasts with angiogenic factors [36] or other types of cells [23] to establish a vasculature network, may be needed to solve this problem. One strategy discussed above, is the combination of a myoblast sheet with omentum tissue that has a rich vasculature network. One report recently demonstrated the effectiveness of this approach for retention of the implanted cell sheets [39]. This report also suggested that the implanted myoblast sheet might induce vasculature connections between arteries of the transplanted omentum and the native coronary arteries, suggesting the possibility of biocoronary artery bypass grafting. This method may also be used in conjunction with iPS cell-derived cardiomyocytes to generate an artificial thick cardiac structure with increased vascular connections.

6. Conclusions

In this review, we surveyed many exciting topics in the area of cell sheet technology for cardiac repair. Owing to these studies, some techniques have already been tested in clinical applications, but the mechanisms by which they improve cardiac function are only partially understood, and much of the technology is still in the early stages of development, both experimentally and in the clinic. Nevertheless, the field of clinical myocardial regenerative therapy holds much promise, and we expect to witness more progress in this innovative technology in the near future.

Conflict of Interests

The authors declare that there is no conflict of interests regarding the publication of this paper.

References

[1] P. Menasché, O. Alfieri, S. Janssens et al., "The myoblast autologous grafting in ischemic cardiomyopathy (MAGIC) trial: first randomized placebo-controlled study of myoblast transplantation," *Circulation*, vol. 117, no. 9, pp. 1189–1200, 2008.

[2] B. E. Strauer, M. Brehm, T. Zeus et al., "Repair of infarcted myocardium by autologous intracoronary mononuclear bone marrow cell transplantation in humans," *Circulation*, vol. 106, no. 15, pp. 1913–1918, 2002.

[3] S. Miyagawa, Y. Sawa, S. Sakakida et al., "Tissue cardiomyoplasty using bioengineered contractile cardiomyocyte sheets to repair damaged myocardium: their integration with recipient myocardium," *Transplantation*, vol. 80, no. 11, pp. 1586–1595, 2005.

[4] K. Nishida, M. Yamato, Y. Hayashida et al., "Corneal reconstruction with tissue-engineered cell sheets composed of autologous oral mucosal epithelium," *The New England Journal of Medicine*, vol. 351, no. 12, pp. 1187–1196, 2004.

[5] A. Kushida, M. Yamato, Y. Isoi, A. Kikuchi, and T. Okano, "A noninvasive transfer system for polarized renal tubule epithelial cell sheets using temperature-responsive culture dishes," *European Cells and Materials*, vol. 10, pp. 23–30, 2005.

[6] T. Shimizu, M. Yamato, A. Kikuchi, and T. Okano, "Two-dimensional manipulation of cardiac myocyte sheets utilizing temperature-responsive culture dishes augments the pulsatile amplitude," *Tissue Engineering*, vol. 7, no. 2, pp. 141–151, 2001.

[7] T. Shimizu, M. Yamato, T. Akutsu et al., "Electrically communicating three-dimensional cardiac tissue mimic fabricated by layered cultured cardiomyocyte sheets," *Journal of Biomedical Materials Research*, vol. 60, no. 1, pp. 110–117, 2002.

[8] T. Shimizu, M. Yamato, Y. Isoi et al., "Fabrication of pulsatile cardiac tissue grafts using a novel 3-dimensional cell sheet manipulation technique and temperature-responsive cell culture surfaces," *Circulation Research*, vol. 90, no. 3, pp. e40–e48, 2002.

[9] T. Shimizu, H. Sekine, Y. Isoi, M. Yamato, A. Kikuchi, and T. Okano, "Long-term survival and growth of pulsatile myocardial tissue grafts engineered by the layering of cardiomyocyte sheets," *Tissue Engineering*, vol. 12, no. 3, pp. 499–507, 2006.

[10] S. Sekiya, T. Shimizu, M. Yamato, A. Kikuchi, and T. Okano, "Bioengineered cardiac cell sheet grafts have intrinsic angiogenic potential," *Biochemical and Biophysical Research Communications*, vol. 341, no. 2, pp. 573–582, 2006.

[11] T. Shirasaka, S. Miyagawa, S. Fukushima et al., "A slow-releasing form of prostacyclin agonist ($ONO_{13}O_1SR$) enhances endogenous secretion of multiple cardiotherapeutic cytokines and improves cardiac function in a rapid-pacing-induced model of canine heart failure," *The Journal of Thoracic Cardiovascular Surgery*, vol. 146, no. 2, pp. 413–421, 2013.

[12] Y. Imanishi, S. Miyagawa, S. Fukushima et al., "Sustained-release delivery of prostacyclin analogue enhances bone marrow-cell recruitment and yields functional benefits for acute myocardial infarction in mice," *PLoS ONE*, vol. 8, no. 7, Article ID e69302, 2013.

[13] N. Dib, R. E. Michler, F. D. Pagani et al., "Safety and feasibility of autologous myoblast transplantation in patients with ischemic cardiomyopathy: four-year follow-up," *Circulation*, vol. 112, no. 12, pp. 1748–1755, 2005.

[14] I. A. Memon, Y. Sawa, N. Fukushima et al., "Repair of impaired myocardium by means of implantation of engineered autologous myoblast sheets," *The Journal of Thoracic and Cardiovascular Surgery*, vol. 130, no. 5, pp. 1333–1341, 2005.

[15] H. Kondoh, Y. Sawa, S. Miyagawa et al., "Longer preservation of cardiac performance by sheet-shaped myoblast implantation in dilated cardiomyopathic hamsters," *Cardiovascular Research*, vol. 69, no. 2, pp. 466–475, 2006.

[16] H. Hata, G. Matsumiya, S. Miyagawa et al., "Grafted skeletal myoblast sheets attenuate myocardial remodeling in pacing-induced canine heart failure model," *The Journal of Thoracic and Cardiovascular Surgery*, vol. 132, no. 4, pp. 918–924, 2006.

[17] Y. Itabashi, S. Miyoshi, S. Yuasa et al., "Analysis of the electrophysiological properties and arrhythmias in directly contacted skeletal and cardiac muscle cell sheets," *Cardiovascular Research*, vol. 67, no. 3, pp. 561–570, 2005.

[18] B. Léobon, I. Garcin, P. Menasché, J.-T. Vilquin, E. Audinat, and S. Charpak, "Myoblasts transplanted into rat infarcted myocardium are functionally isolated from their host," *Proceedings of the National Academy of Sciences of the United States of America*, vol. 100, no. 13, pp. 7808–7811, 2003.

[19] S. Miyagawa, M. Roth, A. Saito, Y. Sawa, and S. Kostin, "Tissue-engineered cardiac constructs for cardiac repair," *Annals of Thoracic Surgery*, vol. 91, no. 1, pp. 320–329, 2011.

[20] Y. Sawa, S. Miyagawa, T. Sakaguchi et al., "Tissue engineered myoblast sheets improved cardiac function sufficiently to discontinue LVAS in a patient with DCM: report of a case," *Surgery Today*, vol. 42, no. 2, pp. 181–184, 2012.

[21] Y. Miyahara, N. Nagaya, M. Kataoka et al., "Monolayered mesenchymal stem cells repair scarred myocardium after myocardial infarction," *Nature Medicine*, vol. 12, no. 4, pp. 459–465, 2006.

[22] H. N. Sabbah, "The cardiac support device and the myosplint: treating heart failure by targeting left ventricular size and shape," *Annals of Thoracic Surgery*, vol. 75, no. 6, pp. S13–S19, 2003.

[23] H. Sekine, T. Shimizu, K. Hobo et al., "Endothelial cell coculture within tissue-engineered cardiomyocyte sheets enhances neovascularization and improves cardiac function of ischemic hearts," *Circulation*, vol. 118, no. 14, pp. S145–152, 2008.

[24] H. Kobayashi, T. Shimizu, M. Yamato et al., "Fibroblast sheets co-cultured with endothelial progenitor cells improve cardiac function of infarcted hearts," *Journal of Artificial Organs*, vol. 11, no. 3, pp. 141–147, 2008.

[25] K. Hobo, T. Shimizu, H. Sekine, T. Shinoka, T. Okano, and H. Kurosawa, "Therapeutic angiogenesis using tissue engineered human smooth muscle cell sheets," *Arteriosclerosis, Thrombosis, and Vascular Biology*, vol. 28, no. 4, pp. 637–643, 2008.

[26] I. A. Memon, Y. Sawa, S. Miyagawa, S. Taketani, and H. Matsuda, "Combined autologous cellular cardiomyoplasty with skeletal myoblasts and bone marrow cells in canine hearts for ischemic cardiomyopathy," *The Journal of Thoracic and Cardiovascular Surgery*, vol. 130, no. 3, pp. 646–653, 2005.

[27] K. Matsuura, A. Honda, T. Nagai et al., "Transplantation of cardiac progenitor cells ameliorates cardiac dysfunction after myocardial infarction in mice," *The Journal of Clinical Investigation*, vol. 119, no. 8, pp. 2204–2217, 2009.

[28] R. Bolli, A. R. Chugh, D. D'amario et al., "Cardiac stem cells in patients with ischaemic cardiomyopathy (SCIPIO): initial results of a randomised phase 1 trial," *The Lancet*, vol. 378, no. 9806, pp. 1847–1857, 2011.

[29] S. Kamata, S. Miyagawa, S. Fukushima et al., "Improvement of cardiac stem cell-sheet therapy for chronic ischemic injury by adding endothelial progenitor cell transplantation: analysis of layer-specific regional cardiac function," *Cell Transplant*, 2013.

[30] K. Takahashi and S. Yamanaka, "Induction of pluripotent stem cells from mouse embryonic and adult fibroblast cultures by defined factors," *Cell*, vol. 126, no. 4, pp. 663–676, 2006.

[31] T. Yu, S. Miyagawa, K. Miki et al., "In vivo differentiation of induced pluripotent stem cell-derived cardiomyocytes," *Circulation Journal*, vol. 77, no. 5, pp. 1297–1306, 2013.

[32] M. Kawamura, S. Miyagawa, K. Miki et al., "Feasibility, safety, and therapeutic efficacy of human induced pluripotent stem cell-derived cardiomyocyte sheets in a porcine ischemic cardiomyopathy model," *Circulation*, vol. 126, pp. S29–S37, 2012.

[33] K. Miki, H. Uenaka, A. Saito et al., "Bioengineered myocardium derived from induced pluripotent stem cells improves cardiac function and attenuates cardiac remodeling following chronic myocardial infarction in rats," *Stem Cells Translational Medicine*, vol. 1, no. 5, pp. 430–437, 2012.

[34] M. Kawamura, S. Miyagawa, S. Fukushima et al., "Enhanced survival of transplanted human induced pluripotent stem cell-derived cardiomyocytes by the combination of cell sheets with the pedicled omental flap technique in a porcine heart," *Circulation*, vol. 128, pp. S87–S94, 2013.

[35] H. Masumoto, T. Matsuo, K. Yamamizu et al., "Pluripotent stem cell-engineered cell sheets reassembled with defined cardiovascular populations ameliorate reduction in infarct heart function through cardiomyocyte-mediated neovascularization," *Stem Cells*, vol. 30, no. 6, pp. 1196–1205, 2012.

[36] S. Miyagawa, Y. Sawa, S. Taketani et al., "Myocardial regeneration therapy for heart failure: hepatocyte growth factor enhances the effect of cellular cardiomyoplasty," *Circulation*, vol. 105, no. 21, pp. 2556–2561, 2002.

[37] P. Menasché, A. A. Hagège, J.-T. Vilquin et al., "Autologous skeletal myoblast transplantation for severe postinfarction left ventricular dysfunction," *Journal of the American College of Cardiology*, vol. 41, no. 7, pp. 1078–1083, 2003.

[38] S. Saito, S. Miyagawa, T. Sakaguchi et al., "Myoblast sheet can prevent the impairment of cardiac diastolic function and late remodeling after left ventricular restoration in ischemic cardiomyopathy," *Transplantation*, vol. 93, no. 11, pp. 1180–1115, 2012.

[39] Y. Shudo, S. Miyagawa, S. Fukushima et al., "Novel regenerative therapy using cell-sheet covered with omentum flap delivers a huge number of cells in a porcine myocardial infarction model," *The Journal of Thoracic and Cardiovascular Surgery*, vol. 142, no. 5, pp. 1188–1196, 2011.

Cardiovascular Research (2013) **99**, 102–110
doi:10.1093/cvr/cvt088

Transplantation of myoblast sheets that secrete the novel peptide SVVYGLR improves cardiac function in failing hearts

Ayako Uchinaka[1], Naomasa Kawaguchi[1,2]*, Yoshinosuke Hamada[1], Seiji Mori[1], Shigeru Miyagawa[3], Atsuhiro Saito[4], Yoshiki Sawa[3], and Nariaki Matsuura[1]

[1]Department of Molecular Pathology, Osaka University Graduate School of Medicine, Suita, Japan; [2]Department of Cardiovascular Pathology, Division of Health Sciences, Osaka University Graduate School of Medicine, Suita, Japan; [3]Department of Cardiovascular Surgery, Osaka University Graduate School of Medicine, Suita, Japan; and [4]Medical Center of Translational Research, Osaka University Hospital, Osaka University Graduate School of Medicine, Suita, Japan

Received 4 December 2012; revised 27 March 2013; accepted 7 April 2013; online publish-ahead-of-print 23 April 2013

Time for primary review: 52 days

Aims Transplantation of myoblast sheets is a promising therapy for enhancing cardiac function after heart failure. We have previously demonstrated that a 7-amino-acid sequence (Ser-Val-Val-Tyr-Gly-Leu-Arg) derived from osteopontin (SV peptide) induces angiogenesis. In this study, we evaluated the long-term therapeutic effects of myoblast sheets secreting SV in a rat infarction model.

Methods and results Two weeks after ligation of the left anterior descending coronary artery, the animals were divided into the following three groups: a group transplanted with wild-type rat skeletal myoblast sheets (WT-rSkMs); a group transplanted with SV-secreting myoblast sheets (SV-rSkMs); and a control group (ligation only). We evaluated cardiac function, histological changes, and smooth muscle actin (SMA) expression through transforming growth factor-β (TGF-β) signalling. The ejection fraction and fractional shortening were significantly better, and the enlargement of end-systolic volume was also significantly attenuated in the SV-rSkM group. Left ventricular remodelling, including fibrosis and hypertrophy, was significantly attenuated in the SV-rSkM group, and SV secreted by the myoblast sheets promoted angiogenesis in the infarcted border area. Furthermore, many clusters of SMA-positive cells were observed in the infarcted areas in the SV-rSkM group. *In vitro* SMA expression was increased when SV was added to the isolated myocardial fibroblasts. Moreover, SV bound to the TGF-β receptor, and SV treatment activated TGF-β receptor–Smad signalling.

Conclusion The SV-secreting myoblast sheets facilitate a long-term improvement in cardiac function. The SV can induce differentiation of fibroblasts to myofibroblasts via TGF-β–Smad signalling. This peptide could possibly be used as a bridge to heart transplantation or as an ideal peptide drug for cardiac regeneration therapy.

Keywords Cell therapy • Peptides • Myocardial infarction • Myofibroblats • Transforming growth factor-β

1. Introduction

In heart failure, tissue damage processes caused by ischaemia, such as cell death, fibrosis, and hypertrophy, gradually progress until the cardiac tissue becomes dysfunctional.[1–3] Transplantation of myoblast sheets is a promising treatment for ischaemic heart failure, and can inhibit left ventricular (LV) remodelling and improve cardiac function via paracrine effectors.[4–8] The cell-sheet technique avoids the arrhythmogenicity associated with skeletal myoblast therapy by injection.[9]

However, this treatment has failed to achieve long-term therapeutic effects, because the transplanted sheets are exposed to blood and nutrient deprivation and drop out from the injured myocardium. Recent studies demonstrated that myoblast sheets that overexpress different cardioprotective agents display enhanced therapeutic effects.[10,11] Therefore, the combined application of gene therapy with angiogenic agents and myoblast sheet transplantation may achieve sustained therapeutic efficacy. Through the secretion of angiogenic factors from transplanted myoblasts, the newly formed blood vessels can supply blood flow to the surviving myocardium and the transplanted

* Corresponding author: 1-7 Yamada-oka, Suita, Osaka 565-0871, Japan. Tel: +81 6 6879 2588; fax: +81 6 6879 2588, E-mail: kawaguch@sahs.med.osaka-u.ac.jp

cells, and the functional deterioration of ischaemic cardiomyopathy should thus improve in the long term.

Osteopontin is a multifunctional cytokine expressed during healing and fibrotic processes.[12] We have previously reported that the osteopontin-derived peptide Ser-Val-Val-Tyr-Gly-Leu-Arg (SVVYGLR; SV) exhibits angiogenic activity *in vitro* and *in vivo*,[13–17] and that its angiogenic activity is as potent as that of vascular endothelial growth factor (VEGF).[14] Owing to their high molecular weights, the most well-known angiogenesis-promoting factors, namely, VEGF and hepatocyte growth factor (HGF), are resistant to degradation. In contrast, peptides such as SV are more easily degraded by peptidase within an organism and show only a few adverse effects, such as oedema and pleural fluid accumulation.[18–20] This indicates the high biocompatibility of peptides.

In this study, we hypothesized that the augmentation of myoblast sheets by SV gene transfer could improve cardiac function in the long term.

2. Methods

2.1 Animal ethics

Animal care complied with the 'Guide for Care and Use of Laboratory Animals' (NIH publication no. 85-23, revised 1996). The Ethics Review Committee for Animal Experimentation of Osaka University Graduate School of Medicine approved the experimental protocols.

2.2 Isolation of skeletal myoblasts and sheets

After induction of general anaesthesia with pentobarbital (300 mg/kg) and heparin (150 U) by intraperitoneal injection, myoblasts were isolated from the skeletal muscle of the tibialis anterior muscle of 3-week-old male Lewis rats. The muscles were minced and enzymatically dissociated with 0.2% collagenase type II (Worthington Biochemical Corp., Lakewood, NJ, USA) and trypsin at 37°C. The isolated cells were suspended in Dulbecco's modified Eagle's medium with 20% fetal bovine serum. After being pre-plated twice, non-adherent cells were then plated on a dish coated with Matrigel (Becton Dickinson Bioscience, Franklin Lakes, NJ, USA) and incubated at 37°C in humidified air enriched with 5% CO_2. We maintained the cell densities at <70% confluence to prevent skeletal myoblast differentiation that would result in myotube formation. Myoblast sheets were formed by plating 3×10^6 infected myoblasts on a temperature-responsive culture dish (UpCell; CellSeed, Tokyo, Japan).

2.3 Animal model and myoblast sheet transplantation

The myocardial infarction (MI) models were generated via ligation of the left anterior descending (LAD) coronary artery in 8-week-old female F344/NJcl-rnu/rnu rats. The rats were anaesthetized by inhalation of isoflurane (2%, 0.2 mL/min), intubated, and placed on a respirator during surgery to maintain ventilation. The carrier gas for isoflurane is oxygen. The adequacy of anaesthesia was monitored by electrocardiography and pulse rate. Two weeks after ligation of the LAD coronary artery, the myoblast sheets were transplanted. The rats were randomly divided into the following three groups: (i) a WT-rat skeletal myoblast (rSkM) group (transplanted with three wild-type myoblast sheets, $n = 6$); (ii) an SV-rSkM group (transplanted with three SV-secreting myoblast sheets, $n = 8$); and (iii) a control group (sham operation, $n = 6$). Each sheet was individually applied to the infarcted area.

2.4 Overexpression and transfection of SV

A lentiviral vector containing the complementary DNA (cDNA) of SV (SV/pCS-CG) was constructed (*Figure 1A*). The cDNA of SV was synthesized using DNA oligonucleotides. The primer sequences were as follows: forward, 1,5′-GCGCCACCATGGAGACAGACACACTCCTGCTATGGGTACTGCTGCTCTGGGTTCCAGGT-3′; forward, 2,5′-TCCACTGGTGACGCGGCCCAGCCGGCCAGTGTGGTTTATGGACTGAGGCTCGAGTACCCATACGATGTTCCAGATTACGCTTAAC-3′; reverse, 1,5′-TCGAGTTAAGCGTAATCTGGAACATCGTATGGGTACTCGAGCCTCAGTCCATAAACCACACT-3′; and reverse, 2,5′-GGCCGGCTGGGCCGCGTCACCAGTGGAACCTGGAACCCAGAGCAGCAGTACCCATAGCAGGAGTGTGTCTGTCTCCATGGTGGCG-3′.

The synthesized DNA oligonucleotides were linked and ligated to pCS-CG, and the isolated rSkMs were infected via incubation for 48 h in the presence of SV/pCS-CG.

2.5 Dot blotting assay

The culture media were used for the assays. Each sample was coated onto a black 96-well microplate overnight. To evaluate the secretion SV volume, the serially diluted solution of SV-HA peptide was also coated onto the plate as a control. After blocking, the primary antibody against the HA tag (Santa Cruz Biotechnology, Santa Cruz, CA, USA) was added to each well. After washing, anti-rabbit IgG-linked horseradish peroxidase (GE Healthcare, Piscataway, NJ, USA) was added. After washing, the plate was exposed to an Enhanced Chemiluminescence (ECL) kit (GE Healthcare).

2.6 Measurement of cardiac function

The cardiac function of the treated rats was evaluated by echocardiography 2, 4, 6, and 8 weeks after sheet transplantation. Baseline measurements were

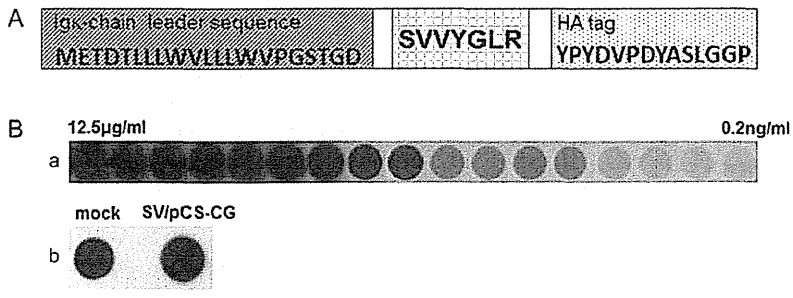

Figure 1 Assessment of SV expression. (*A*) View showing the frame format of the constructed SV gene. (*B*) Expression of SV in rSkMs infected with SV/pCS-CG by dot blotting: (*a*) the dilution series of SV-HA peptide; and (*b*) control cells infected with the empty vector (mock, left) and rSkMs infected with SV/pCS-CG (right).

made before sheet transplantation. The measurements were made using a SONOS 5500 sonograph (Philips Electronics, Tokyo, Japan) with a 12 MHz transducer under general anaesthesia induced and maintained by inhalation of isoflurane (2%, 0.2 mL/min) as mentioned above. The LV end-systolic area, LV end-diastolic area, and LV dimensions at end diastole and end systole (LVIDd and LVIDs, respectively) were determined. The ejection fraction (EF), fractional shortening (FS), end-diastolic volume (EDV), and end-systolic volume (ESV) were calculated as follows:

$$\text{LVEF (\%)} = (\text{LVDd}^3 - \text{LVDs}^3)/\text{LVDd}^3 \times 100\ (\%)$$
$$\text{LV\%FS} = [(\text{LVDd} - \text{LVDs})/\text{LVDd}] \times 100\ (\%)$$
$$\text{EDV} = \text{LVIDd}^3 \times (0.98 \times \text{LVIDd} + 5.90)\ (\text{mL})$$
$$\text{ESV} = \text{LVIDs}^3 \times (1.14 \times \text{LVIDs} + 4.18)\ (\text{mL})$$

2.7 Heart weight/body weight ratio

The body weights (BW; in grams) of the rats were measured 8 weeks after sheet transplantation, after which the rats were anaesthetized with pentobarbital (300 mg/kg) and heparin (150 U) by intraperitoneal injection, and their hearts were rapidly removed and weighed (in milligrams). The heart weight (HW)/BW ratio was then calculated.

2.8 Histological analyses

Myocardial specimens were obtained 8 weeks post-transplantation. The formalin-fixed samples were embedded in paraffin. The LV chamber diameter and the anterior wall thickness were measured from sections stained with haematoxylin and eosin. Infarcted wall thickness, posterior wall thickness, and LV chamber diameter were measured with the scale loupe. The sections were evaluated morphologically using the NIS Elements system (Nikon, Tokyo, Japan). Sirius Red staining was used to detect fibrosis. The percentage of fibrosis was calculated from the fibrotic ratio in the infarct border area. Periodic acid–Schiff staining for cardiomyocyte hypertrophy was also performed. We randomly selected 100 cardiomyocytes and measured the two-point shortest axes at the level of the nucleus.

Immunohistochemical staining for von Willebrand factor antigen was used to label vascular endothelial cells to permit the counting of blood vessels. The sections were incubated with primary antibody against von Willebrand factor (rabbit polyclonal; Dako, Glostrup, Denmark). The sections were incubated with a biotinylated anti-rabbit IgG antibody (Dako) and further incubated with peroxidase-conjugated streptavidin (SA; GE Healthcare). Visualization was performed with biphenyl-3,3′,4,4′-tetramine solution (Sigma, St Louis, MO, USA). The stained vascular endothelial cells were counted under a light microscope.

The distribution of myofibroblast-like cells was evaluated by immunohistochemical staining with anti-smooth muscle actin (SMA) antibody (Dako) and anti-smooth muscle myosin heavy chain (SM-MHC) type 2 antibody (Abcam Ltd, Cambridge, UK). The SMA-positive cell density was calculated as SMA positive area/infarcted area × 100 (%).

2.9 Primary culture of adult ventricular fibroblasts

Cardiac fibroblasts (CFs) were isolated from 8-week-old adult male Sprague–Dawley rats 4 weeks after the induction of MI by LAD ligation. The hearts were excised from anaesthetized rats and quickly transferred to Hank's buffered salt solution. The minced left ventricular tissues were digested using 100 U/mL type II collagenase and 0.1% trypsin at 37°C. The cells were centrifuged and suspended in Dulbecco's modified Eagle's medium supplemented with 10% fetal bovine serum, and incubated at 37°C in humidified air enriched with 5% CO_2.

2.10 Immunofluorescence staining

The isolated fibroblasts were incubated with SV (10 μg/mL), SV random peptide (GYRVLSV; 10 μg/mL), or transforming growth factor-β1 (TGF-β1; 25 ng/mL) for 72 h. The cells were fixed with 4% paraformaldehyde and incubated with anti-SMA antibody followed by incubation with cyanine-3-conjugated anti-rabbit secondary antibody (GE Healthcare). The nuclei were stained with 4′,6-diamino-2-phenylindole (DAPI; Invitrogen Life Technologies, Grand Island, NY, USA), and the fluorescent signals were detected by fluorescence microscopy (ECLIPSE E600, Nikon).

2.11 Western blotting assay

The isolated fibroblasts were incubated with SV (10 μg/mL), SV random peptide (10 μg/mL), or TGF-β1 (25 ng/mL) for 72 h. The cells were suspended in lysis buffer (50 mM Tris at pH 8.0, 120 mM NaCl, 1 mM EDTA, and 0.5% Nonidet P-40). Proteins in whole-cell lysates were separated by SDS–PAGE, transferred to a polyvinylidene fluoride transfer membrane (Millipore, Billerica, MA, USA), and probed sequentially with antibodies against SMA and α-tubulin (Sigma). The blots were developed using an ECL kit.

To examine the activity of TGF-β receptor–Smad signalling induced by SV, the phosphorylation of Smad2, Smad3, and TGF-β receptor I (TβRI) was studied by western blotting. The isolated fibroblasts were incubated with SV (10 μg/mL), SV random peptide (10 μg/mL), or TGF-β1 (25 ng/mL) for 1 h. Primary antibodies against phospho-Smad2, phospho-Smad3, Smad2/3 (Cell Signaling Technology, Inc., Danvers, MA, USA), TβRI (phospho S165; Abcam), and α-tubulin were used.

2.12 Construction of recombinant transforming growth factor-β receptorII

A pcDNA3.1 vector containing the cDNA encoding TβRII (pcDNA3.1-TβRII) was constructed. The recombinant TβRII was produced by transfecting HEK 293T cells with pcDNA3.1-TβRII. The culture media containing recombinant TβRII were harvested. The purification of recombinant TβRII was done using immunoprecipitation with anti-TβRII antibody.

2.13 Biacore analysis

The binding of SV to TβRII was assessed by Biacore analysis. Biotinylated SVs were captured on SA-coated BIAcore SA sensor chips (GE Healthcare, Piscataway, NJ, USA). Ligands were diluted to 10 μg/mL and injected at 10 μL/mL. To correct for refractive index change, non-specific binding, and instrument drift, a reference flow cell contained the SA-coated surface only. The recombinant TβRII was diluted to 10 μg/mL in Hank's buffered salt solution and injected during the association phase for 5 min (30 μL/min).

2.14 *In situ* proximity ligation assay

The Duolink *in situ* proximity ligation assay (PLA; Olink Biosciences, Uppsala, Sweden) was performed according to the manufacturer's protocol. The isolated fibroblasts were incubated in the presence of SV-HA peptide or SV-HA random peptide (GYRVLSV; 1 μg/mL) for 1 h. The fixed fibroblasts were incubated with the following primary antibodies: rabbit polyclonal anti-TβRII (Abcam) and mouse monoclonal anti-HA (Nacalai Tesque). The cells were then incubated with PLA probes consisting of two secondary anti-rabbit and anti-mouse antibodies, each tagged with an oligonucleotide. A hybridization solution consisting of two oligonucleotide linkers complementary to each PLA probe was added to the cells. The isolated cells were incubated with a Duolink Ligation stock containing ligase and Duolink polymerase. In addition, the cells were incubated with a detection solution consisting of fluorescently labelled oligonucleotides that hybridize to the rolling circle amplification product. The PLA signal was visualized using fluorescence microscopy.

2.15 Statistical analyses

Data are presented as the means ± SEM. Cardiac function was analysed by repeated-measures analysis of variance (ANOVA) for differences across the entire time course, as well as one-way ANOVA, whereas the Tukey–Kramer *post hoc* test was used to examine significant differences at each time point. To assess the significance of the differences between individual groups for

other data, statistical comparisons were performed using Student's unpaired *t*-test. $P < 0.05$ was considered statistically significant.

3. Results

3.1 Overexpression of SV in rat skeletal myoblasts

The signal strength of dots in wells coated with the culture medium of SV/pCS-CG-infected rSkMs was stronger than that of dots in wells coated with the culture medium of mock-infected rSkMs (*Figure 1B*[*b*]). The SV was synthesized and secreted by SV/pCS-CG-infected rSkMs. In addition, from the dilution series of SV-HA peptide, the secretion volume of SV was calculated to be approximately 3.125–6.25 ng/mL (*Figure 1B*[*a*]).

3.2 Effect of SV-secreting myoblast sheet on left ventricular function

Echocardiography revealed significantly better values of LVEF and %FS in the WT-rSkM and SV-rSkM groups compared with the control group at all time points after transplantation ($P < 0.01$). Although there were still significant differences between the control and WT-rSkM groups after the 4 week time point, the LVEF and %FS in the WT-rSkM group decreased dramatically. Furthermore, LVEF and %FS were significantly better in the SV-rSkM group at 2, 6, and 8 weeks after transplantation compared with the WT-rSkM group (2 and 6 weeks, $P < 0.05$; 8 weeks, $P < 0.01$; *Figure 2A* and *B*).

The evaluation of LVIDs illustrated the inhibition of dilatation in the SV-rSkM group in comparison with the control and WT-rSkM groups. In particular, at 6 and 8 weeks after transplantation LVIDs was significantly attenuated in the SV-rSkM group compared with the control group (6 weeks $P < 0.05$; 8 weeks $P < 0.01$; *Table 1*). The enlargement of ESV was also significantly attenuated in the SV-rSkM group compared with the control group at 6 and 8 weeks after transplantation (6 weeks, $P < 0.05$; 8 weeks, $P < 0.01$; *Table 1*). The increase in EDV was significantly inhibited in the SV-rSkM group compared with the control group only at 8 weeks after transplantation ($P < 0.05$; *Table 1*).

3.3 Heart weight/body weight ratio

We used the HW/BW ratio as an indicator of cardiac hypertrophy. The HW/BW ratio was significantly greater in the SV-rSkM group at 8 weeks after transplantation compared with the control and WT-rSkM groups ($P < 0.01$; *Figure 2C*).

3.4 Effect of SV-secreting myoblast sheet on left ventricular remodelling

Haematoxylin and eosin staining demonstrated thinning of the infarcted wall in the control and WT-rSkM groups, whereas the thickness of the infarcted wall was maintained in the SV-rSkM group (*Figure 2D* and *Table 2*). Statistical analysis demonstrated that the LV chamber of the SV-rSkM group was significantly less dilated that those of the control and WT-rSkM groups ($P < 0.05$; *Table 2*) and that the infarcted wall in the SV-rSkM group was significantly thicker than that in the control

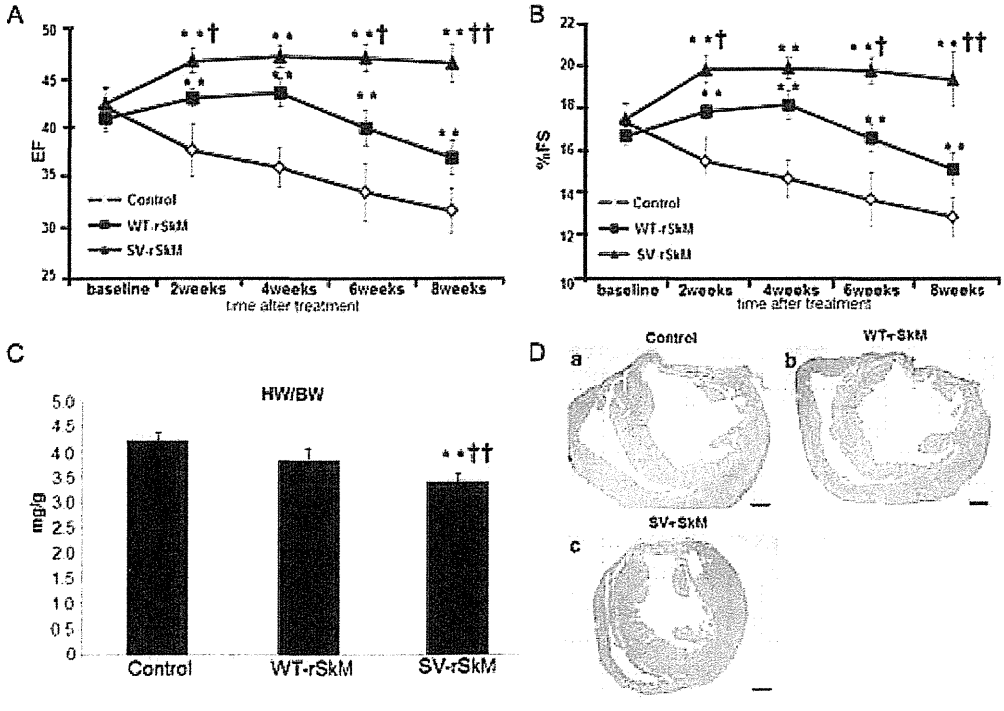

Figure 2 Echocardiographic evaluation of LV function after sheet transplantation (*A*, EF; *B*, %FS). $^{**}P < 0.01$ vs. Control group. $^{\dagger}P < 0.05$, $^{\dagger\dagger}P < 0.01$ vs. WT-rSkM group. Baseline is time of transplantation, which was 2 weeks after ligation of the LAD. Other times in weeks are post-transplantation. (*C*) Evaluation of HW/BW. $^{**}P < 0.01$ vs. Control group. $^{\dagger}P < 0.05$, $^{\dagger\dagger}P < 0.01$ vs. WT-rSkM group. (*D*) Haematoxylin- and eosin-stained section of the left ventricle: (*a*) control; (*b*) WT-rSkM; and (*c*) SV-rSkM (×10 magnification, scale bars represent 1000 μm).

Table 1 Assessment of LVIDd, LVIDs, EDV, and ESV over time by echocardiography

	Baseline	2 weeks	4 weeks	6 weeks	8 weeks
LVIDd (cm)					
Control	0.75 ± 0.04	0.77 ± 0.07	0.81 ± 0.05	0.87 ± 0.04	0.89 ± 0.01
WT-rSkM	0.76 ± 0.02	0.77 ± 0.04	0.80 ± 0.06	0.84 ± 0.06	0.85 ± 0.03
SV-rSkM	0.71 ± 0.05	0.78 ± 0.07	0.78 ± 0.07	0.83 ± 0.03	0.84 ± 0.03*
LVIDs (cm)					
Control	0.63 ± 0.02	0.67 ± 0.05	0.70 ± 0.05	0.75 ± 0.04	0.77 ± 0.02
WT-rSkM	0.63 ± 0.02	0.64 ± 0.03	0.67 ± 0.06	0.69 ± 0.05	0.72 ± 0.04
SV-rSkM	0.64 ± 0.04	0.65 ± 0.05	0.67 ± 0.04	0.67 ± 0.03*	0.69 ± 0.04**
EDV (ml)					
Control	2.87 ± 0.46	3.19 ± 0.93	3.65 ± 0.71	4.46 ± 0.63	4.79 ± 0.26
WT-rSkM	2.93 ± 0.24	3.04 ± 0.43	3.53 ± 0.77	4.05 ± 0.89	4.22 ± 0.54
SV-rSkM	2.77 ± 0.53	3.26 ± 0.70	3.37 ± 0.64	3.92 ± 0.43	4.08 ± 0.43*
ESV (ml)					
Control	1.20 ± 0.13	1.49 ± 0.36	1.71 ± 0.34	2.16 ± 0.40	2.34 ± 0.23
WT-rSkM	1.25 ± 0.14	1.28 ± 0.16	1.53 ± 0.37	1.69 ± 0.33	1.88 ± 0.22
SV-rSkM	1.29 ± 0.21	1.39 ± 0.27	1.48 ± 0.25	1.51 ± 0.23*	1.61 ± 0.25**

Abbreviations: EDV, end-diastolic volume; ESV; end-systolic volume; LVIDd, left ventricular dimensions at end diastole; LVIDs, left ventricular dimensions at end systole. Baseline is the time of transplantation, which was 2 weeks after ligation of the left anterior descending coronary artery; other times in weeks are post-transplantation. *$P < 0.05$, **$P < 0.01$ vs. control group at each time point.

and WT-rSkM groups ($P < 0.01$; *Table 2*). The values of the LV chamber diameter/posterior wall thickness were significantly lower in the SV-rSkM group compared with those in the control and WT-rSkM groups ($P < 0.01$; *Table 2*). There were no significant differences between the control and WT-rSkM groups regarding these indices.

The SV-rSkM group exhibited a significantly lower percentage of fibrosis than the control and WT-rSkM groups in the infarcted border area ($P < 0.01$; *Figure 3A*). The diameters of cardiomyocytes in the SV-rSkM group were significantly smaller than those in the control and WT-rSkM groups ($P < 0.01$; *Figure 3B*). There was no significant difference in the area remote from the transplant among the three groups.

3.5 The pro-angiogenic effects of SV

The capillary density 8 weeks after transplantation was significantly higher in the WT-rSkM and SV-rSkM groups than in the control group ($P < 0.01$). Furthermore, the capillary density in the SV-rSkM group was significantly higher than that in the WT-rSkM group ($P < 0.01$; *Figure 3C[a]–C[c]* and *D*). There was no significant difference in the area remote from the transplant among the three groups.

3.6 The accumulation of smooth muscle actin-positive and smooth muscle myosin heavy chain type2-positive cells by SV

Immunohistochemical staining with an anti-SMA antibody revealed that many clusters of SMA-positive cells were present in infarcted areas in the SV-rSkM group (*Figure 3E*). Statistical analysis indicated that the SMA-positive cell density was significantly higher in the WT-rSkM and SV-rSkM groups than in the control group (WT-rSkM , $P < 0.05$; SV-rSkM, $P < 0.01$; *Figure 3F*). Furthermore, the SMA-positive cell density was significantly higher in the SV-rSkM group than in the WT-rSkM group ($P < 0.05$; *Figure 3F*). Notably, SM-MHC type 2-positive cells were also detected in infarcted areas in the SV-rSkM group, whereas those cells were scarce in the control and WT-rSkM groups (*Figure 3G*).

Table 2 Thickness of the infarcted wall and posterior wall and left ventricular chamber diameter

	Control	WT-rSkM	SV-rSkM
Left ventricular chamber diameter (mm)	4.50 ± 0.46	4.48 ± 0.42	3.85 ± 0.29**††
Infarcted wall thickness (mm)	0.53 ± 0.05	0.51 ± 0.08	0.63 ± 0.06
Posterior wall thickness (mm)	2.04 ± 0.10	1.88 ± 0.25	1.96 ± 0.14
Percentage anterior wall thickness	25.98 ± 2.66	27.20 ± 2.63	32.29 ± 0.98**††
Left ventricular chamber diameter/ posterior wall thickness	2.36 ± 0.22	2.30 ± 0.15	1.98 ± 0.16**††

The percentage anterior wall thickness is the infarcted wall thickness/posterior wall thickness × 100. **$P < 0.01$ vs. control group. ††$P < 0.01$ vs. WT-rSkM group.

3.7 The induction of smooth muscle actin by SV

Expression of SMA was increased when SV was added to the isolated fibroblasts (*Figure 4A* and *B*). The expression level of SMA was similar to that of TGF-β1 (*Figure 4B*). Conversely, the expression level of SMA was unchanged by the addition of SV random peptide (*Figure 4A* and *B*).

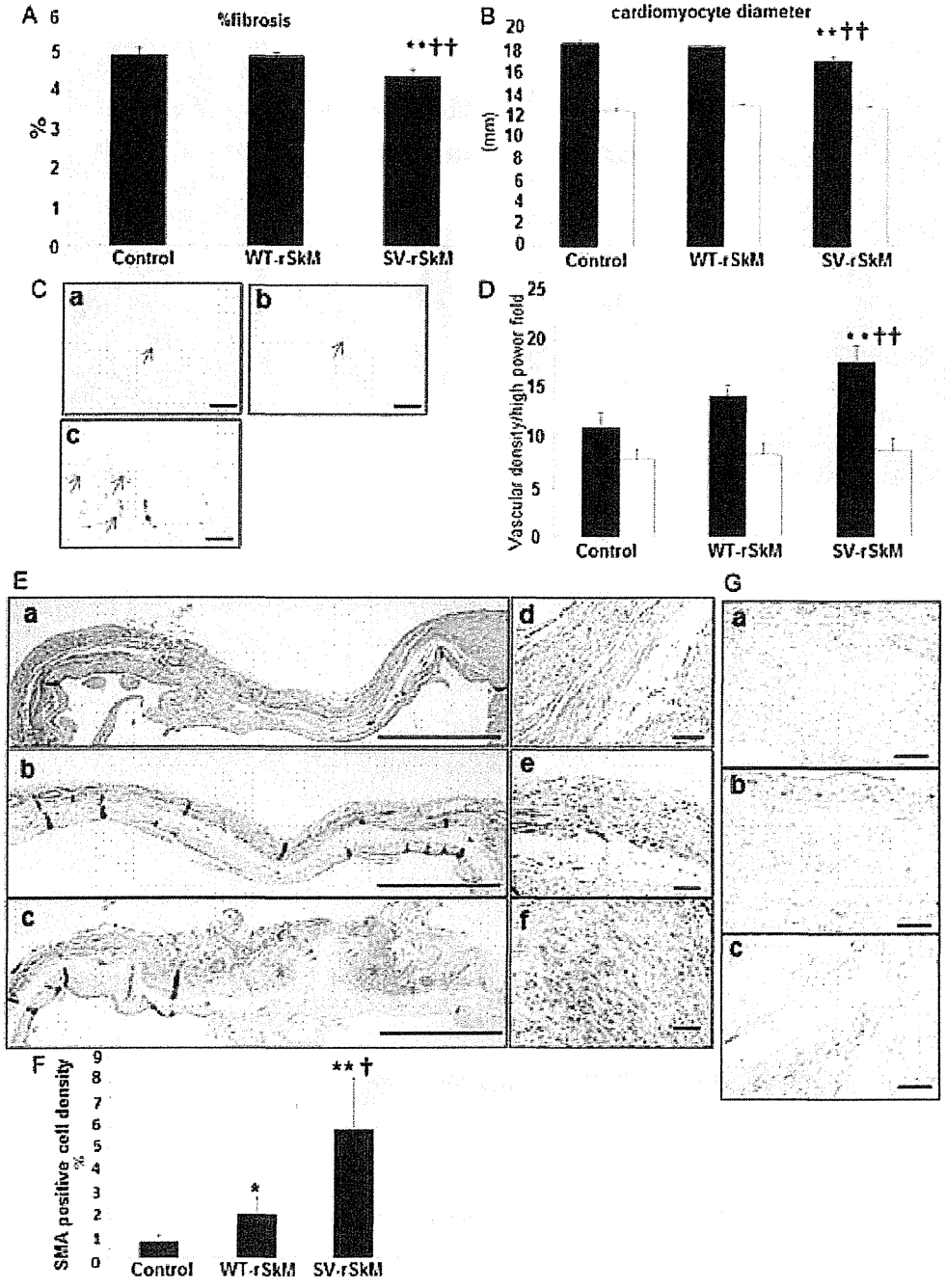

Figure 3 Histological evaluations of LV remodelling. (*A*) Percentage fibrosis. (*B*) Cardiomyocyte diameter. $^{**}P < 0.01$ vs. Control group. $^{\dagger\dagger}P < 0.01$ vs. WT-rSkM group. Filled bars, border area; open bars, remote area. Immunohistochemical staining. (*C*) A section of the infarcted border zone stained with an antibody against von Willebrand factor: (*a*) control; (*b*) WT-rSkM; and (*c*) SV-rSkM (×200 magnification, scale bars represent 100 μm). Newly formed vessel is stained brown. (*D*) Quantitative estimation of vascular density. $^{**}P < 0.01$ vs. Control group. $^{\dagger\dagger}P < 0.01$ vs. WT-rSkM group. Filled bars, border area; open bars, remote area. (*E*) The distribution of SMA-positive cells: (*a*) control; (*b*) WT-rSkM; (*c*) SV-rSkM (*a–c*, ×20 magnification, scale bars represent 1000 μm; e and *f*, ×200 magnification, scale bars represent 100 μm). Red asterisks denote SMA-positive cells. (*F*) Quantitative estimation of the SMA-positive cell density. $^{*}P < 0.05$, $^{**}P < 0.01$ vs. Control group. $^{\dagger}P < 0.05$ vs. WT-rSkM group. (*G*) The distribution of SM-MHC type 2-positive cells: (*a*) control; (*b*) WT-rSkM; and (*c*) SV-rSkM (*a–c*, ×200 magnification, scale bars represent 100 μm).